NRL Memorandum Report 4787

A Compact HF Antenna Array Using Reactively-Terminated Parasitic Elements for Pattern Control

E. J. DINGLE AND W. D. MEYERS

Transmission Technology Branch
Information Technology Division

May 11, 1982

NAVAL RESEARCH LABORATORY
Washington, D.C.

DISCLAIMER NOTICE

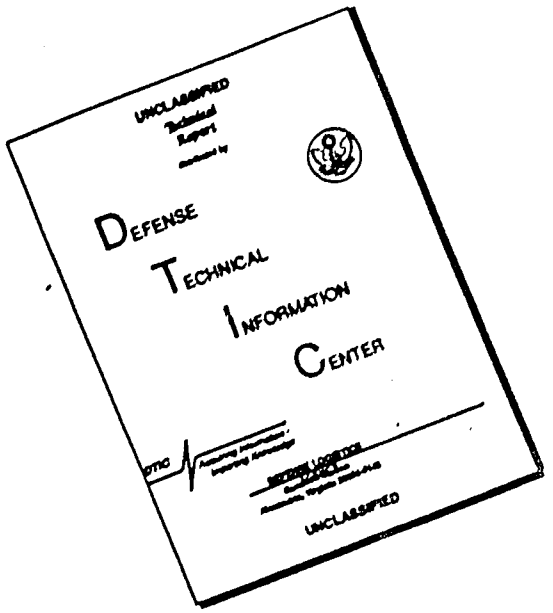

THIS DOCUMENT IS BEST QUALITY AVAILABLE. THE COPY FURNISHED TO DTIC CONTAINED A SIGNIFICANT NUMBER OF PAGES WHICH DO NOT REPRODUCE LEGIBLY.

SECURITY CLASSIFICATION OF THIS PAGE (When Data Entered)

REPORT DOCUMENTATION PAGE		READ INSTRUCTIONS BEFORE COMPLETING FORM
1. REPORT NUMBER NRL Memorandum Report 4797	2. GOVT ACCESSION NO. AD-A114 557	3. RECIPIENT'S CATALOG NUMBER
4. TITLE (and Subtitle) A COMPACT HF ANTENNA ARRAY USING REACTIVELY-TERMINATED PARASITIC ELEMENTS FOR PATTERN CONTROL		5. TYPE OF REPORT & PERIOD COVERED Interim report on a continuing NRL problem. 6. PERFORMING ORG. REPORT NUMBER
7. AUTHOR(s) R.J. Dinger and W.D. Meyers		8. CONTRACT OR GRANT NUMBER(s)
9. PERFORMING ORGANIZATION NAME AND ADDRESS Naval Research Laboratory Washington, DC 20375		10. PROGRAM ELEMENT, PROJECT, TASK AREA & WORK UNIT NUMBERS 61153N; RR021-05-42; 75-0145-0-1
11. CONTROLLING OFFICE NAME AND ADDRESS		12. REPORT DATE May 11, 1982 13. NUMBER OF PAGES 35
14. MONITORING AGENCY NAME & ADDRESS(if different from Controlling Office)		15. SECURITY CLASS. (of this report) UNCLASSIFIED 15a. DECLASSIFICATION/DOWNGRADING SCHEDULE

16. DISTRIBUTION STATEMENT (of this Report)

Approved for public release; distribution unlimited.

17. DISTRIBUTION STATEMENT (of the abstract entered in Block 20, if different from Report)

18. SUPPLEMENTARY NOTES

19. KEY WORDS (Continue on reverse side if necessary and identify by block number)

HF	Adaptive arrays
Antenna arrays	Spatial interference cancellation

20. ABSTRACT (Continue on reverse side if necessary and identify by block number)

Measurements have been made on two 7 element azimuthally-symmetric arrays, consisting of one active receiving element mounted at the center of six symmetrically positioned parasitic elements with variable reactive terminations. The measurements were made at frequencies between 15 and 25 MHz on an antenna range. Most of the data was taken on an array of diameter 80 cm (0.05λ at the center frequency of 18 MHz) with

(Continues)

DD FORM 1 JAN 73 1473 EDITION OF 1 NOV 65 IS OBSOLETE
S/N 0102-014-6601

SECURITY CLASSIFICATION OF THIS PAGE (When Data Entered)

20. ABSTRACT (Continued)

helically-wound monopole elements. Attempts were made to form the array pattern deterministically by using Harrington's theory to compute the reactive loads necessary to form a pattern lobe in a desired direction. Although the pattern lobe could be steered in the general desired direction, the directivity of the pattern was low and reproducibility poor. The majority of the measurements used the array in an adaptive mode in which the reactive terminations were adjusted manually to minimize one or two incident signals representing undesired interference. The manual adaptation consistently produced sharp spatial notches in the direction of the interference in an otherwise nearly omnidirectional pattern. The notches typically had a width of 50 degrees and a depth of 25 to 30 dB below the pattern main lobe; the cancellation bandwidth was 40 kHz.

CONTENTS

A COMPACT HF ANTENNA ARRAY USING REACTIVELY-TERMINATED PARASITIC ELEMENTS FOR PATTERN CONTROL

I. INTRODUCTION

The element spacing of an antenna array is typically a half-wavelength ($\lambda/2$) or more to avoid strong mutual coupling between the elements. When attempts are made to decrease the spacing to $\lambda/4$ and less, the strong mutual coupling causes the array radiation pattern to become very sensitive to the phase and amplitude weights. In addition, the array bandwidth narrows.

This report describes an array operating in the high frequency (HF, 3-30 MHz) band that has elements intentionally spaced close to each other (element spacing of $\sim 0.03\lambda$). The array, termed a reactively steered array, consists of one element that is physically connected to a receiver by a transmission line; the remaining elements serve as parasitic elements coupled to the receiving element by the mutual impedance between the antennas. The array antenna pattern is formed by adjusting the values of the reactances that terminate the parasitic elements. The value of each terminating reactance determines the phase of the incident signal reflected from that parasitic element to the receiving element. Thus, the receiving antenna element "sums" the various reflected signals to form an array output.

The basic concept and theory of a reactively steered array was first described by Harrington [1], but the use of closely-coupled parasitic elements for pattern control dates back to the Yagi-Uda array [2]. This report is concerned primarily with experimental results obtained in the HF band, and the theory of the array is only briefly discussed.

The experimental array discussed below is an azimuthally symmetric array, with the active receiving element mounted at the center of six symmetrically placed parasitic elements. Two types of elements were used: standard $\lambda/4$ monopole whips, and transversely-excited small diameter helixes. The emphasis of the pattern adjustment and control techniques discussed below is on the placement of pattern nulls in the direction of interferers, rather than the steering of a narrow lobe towards a desired signal. This emphasis most accurately reflects the need for a shipboard HF receiving antenna that is omni-directional for desired signals with directive notches for both intentional and unintentional interference. However, some initial attempts were made to adjust the reactances to produce a steered main lobe by calculating the required reactances using Harrington's theoretical expressions and then setting these values on the terminal reactances. Although the results of this effort were largely disappointing, the procedures and data are discussed below.

Manuscript submitted February 22, 1982.

A few of the experimental results in this report were included in a recent paper [3] that in the main discussed a reflection coefficient and transmission line theory approach to describing the behavior of the reactively steered array. Reference 3 also discussed the possibility of providing gain in the terminating load so that any arbitrary complex impedance can be applied (not just reactive). The results in this report are restricted to passive, reactance only control of the terminating loads.

The results reported here demonstrate that very small and compact arrays can be fabricated that are capable of accurately placing narrow pattern minima in the direction of interferers. Using a six element array whose diameter is only 80 cm (corresponding to 0.05λ at the 18 MHz center frequency of the array), minima with a width of 20 degrees and a depth of 25 to 30 dB below the pattern main lobe could be formed in the direction of two interferers. The interferers could be cancelled in this manner over a bandwidth of at least 40 kHz. All adaptation of the array to the incident signals was performed manually, but we have developed an algorithm that should allow rapid automatic adaptation when implemented on a microcomputer.

This report is organized as follows. In Section II we briefly discuss the theory of the array using a mutual impedance approach due to Harrington. After describing the design and fabrication of the two tested arrays in Section III, we give the results of measurements on a quarter-wavelength monopole array using deterministic pattern adjustment in Section IV. In Section V we present the results of manual adaptive adjustment of the arrays. In Section VI we describe an algorithm for control of a reactively steered array, and in Section VII we summarize our results and give recommendations for further work.

II. THEORY

Harrington and his co-workers have described the theory of reactively steered antenna arrays in a paper [1] and several reports [4-6]. Here, we only briefly summarize the theory.

Figure 1 shows a seven-element circular array of reactively loaded monopoles. Viewing the antenna array as an N-port network, the terminal equation can be written

$$\vec{V} = [\, Z_A \,]\ \vec{I} \tag{1}$$

where V and I are the column vectors of the port voltages and currents. For the case of a voltage source at port 1 and all other ports reactively terminated, this equation reduces to

$$\vec{V_a} = [\, Z_A + Z_L \,]\ \vec{I} \tag{2}$$

where

$$\vec{V_a} = (V_o,\ 0,\ \ldots)^T$$

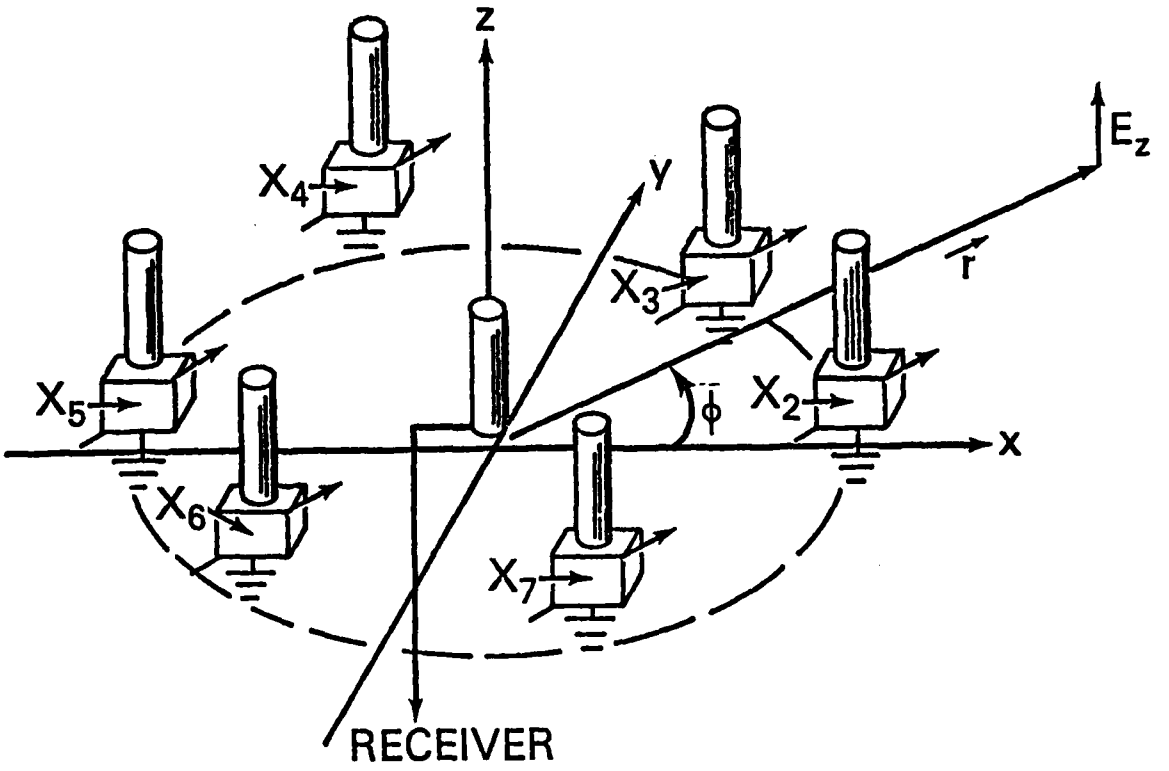

Fig. 1 — 7-Element circular array geometry

and where

$$[Z_L] \begin{bmatrix} 0 & 0 & . & . & . & 0 \\ 0 & jX_L^{(2)} & & & & 0 \\ . & . & & & & \\ . & . & & & & \\ . & . & & & & jX_L^{(N)} \end{bmatrix} \tag{2}$$

where $jX_L^{(1)} = 0$ for the central monopole. The voltage excitation is confined only to the central monopole, so that $\vec{V}^{oc}$ is given by

$$\vec{V}^{oc} = (V_o \; 0 \; 0 \; \cdots)^T \tag{3}$$

where the T indicates transpose.

The far electric field at a distance r generated by the N monopoles in the ϕ direction (ϕ = azimuthal angular coordinate) in the plane of the ground screen (i.e., in the plane $\theta = 90^o$, where θ is the polar angle) is

$$E_Z(\phi) = - \frac{j\eta}{2\pi} \frac{e^{-jkr}}{r} \sum_{n=1}^{N} I_n \, e^{j k(X_n \cos \phi + y_n \sin \phi)} \tag{4}$$

in which x_n and y_n are the monopole element coordinates measured from the selected phase center of the array (in our case, at the center element), and η is the intrinsic impedance of free space. The currents I_n are obtained from Eq. (1) and (3) as

$$I_n = \{ [Z_A + Z_L]^{-1} \}_{1n} V_o \tag{5}$$

where $\{1n\}$ denotes the 1n element of the matrix $[Z_A + Z_L]^{-1}$.

Our main interest is in the array antenna pattern, which is given by

$$F(\phi) = \frac{2\pi r}{\eta I_o} |E_Z(\phi)| \tag{6}$$

where I_o is an arbitrary normalizing current that can be set equal to unity. Substituting Eq. (5) into Eq. (4) and using Eq. (6) yields the equation

$$F(\phi) = \frac{V_o}{I_o} \left| \sum_{n=1}^{N} \{ [Z_A + Z_L]^{-1} \}_{1n} e^{j k(X_n \cos\phi + y_n \sin\phi)} \right| \tag{7}$$

for the array antenna pattern. For a receiving array, the receiver output is proportional to $F(\phi)$ for an incident planewave at an angle ϕ .

A possible technique for forming a given antenna pattern, described by Luzwick and Harrington [6], consists of using P points from a desired pattern $f_o(\phi)$ and minimizing the error given by

$$\epsilon = \sum_{p=1}^{P} W_p \left| |F(\phi_p)| - |f_o(\phi_p)| \right|^2 \qquad (8)$$

in which W_p is a weighting coefficient. The optimum values of the reactive loads (that is, those values that minimize ϵ) can be found by using such schemes as the Rosenbrock algorithm [7] as a strategy to vary the reactive loads that appear in $F(\phi)$. We will describe several attempts to use this approach below and will show that although the required values of the reactive loads can be derived in this manner, there are practical difficulties in setting these values of the loads with sufficient precision to form the desired pattern.

III. EXPERIMENTAL ARRAYS

The two experimental arrays described below were evaluated at the Naval Research Laboratory's Brandywine Antenna Range (BAR), using the setup shown in Fig. 2. The BAR has a platter to rotate the array under test for obtaining antenna patterns and has a large ground screen (diameter of 190 m) to minimize the effects of edge discontinuities at HF. Up to three sources were placed in the far field at the edge of the ground screen (95 m distant) during the various interference cancellation trials. To measure the array pattern, one of the sources was used as a test signal, and the array was rotated synchronously with a polar plotter. All recording and processing equipment was located in an underground room directly beneath the platter.

Quarter-Wavelength ($\lambda/4$) Monopole Array

This array consisted of seven whip antennas, each with a diameter of 1.3 cm and height of 3.5 m. The resonant frequency of the elements was 21 MHz. One central element connected to an HF receiver was surrounded by the six parasitic elements symmetrically positioned on a circle 3.6 m in radius ($\lambda/4$ at 21 MHz). The base of each parasitic element was terminated in the load circuit shown in Fig. 3. The inductor had an air core with a roller contact, and the capacitor was an adjustable air gap type. All adjustments of the capacitors and inductors were performed manually.

Helical Element Array

The helical element was constructed by uniformally winding copper wire on a 5 cm diameter Melamine tube with a pitch of 1 cm over a length of 1.0 m. A 30 cm length of straight copper wire was then added to the top of this element to provide top loading. The measured impedance of the element is shown in Fig. 4. The pole in the impedance at 28.5 MHz is caused by a series resonance of the winding inductance and interwinding capacitance.

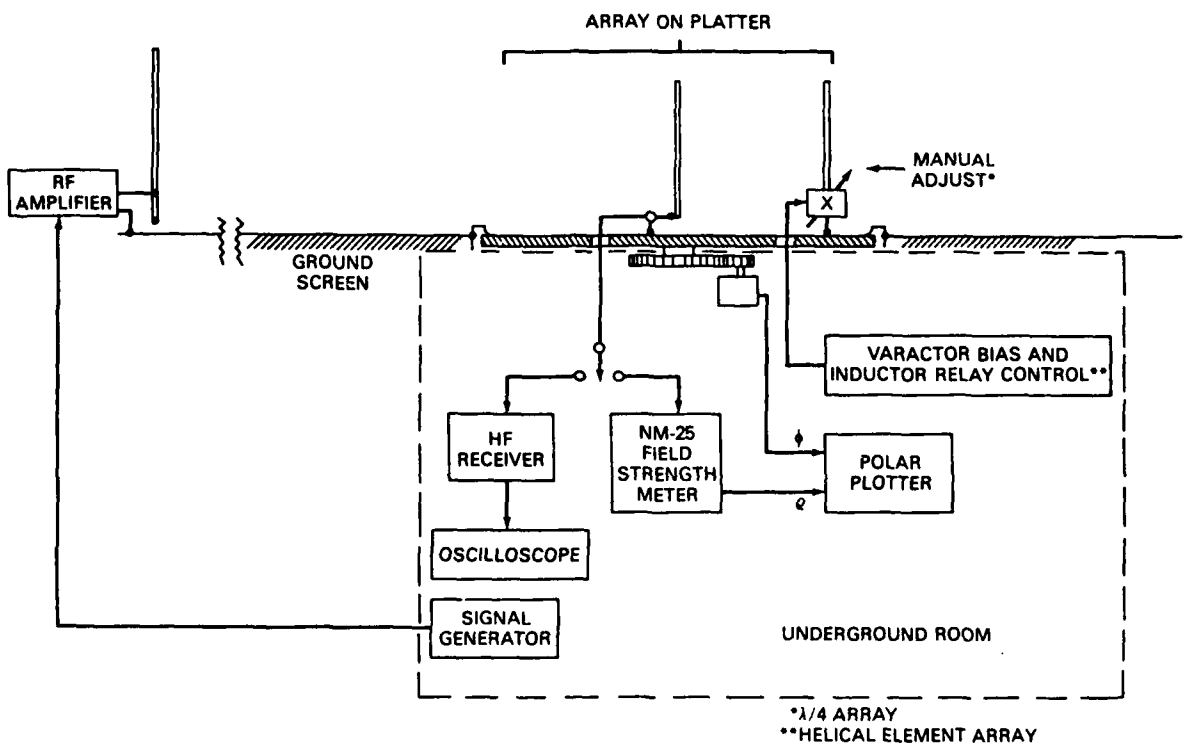

Fig. 2 — Antenna array test setup

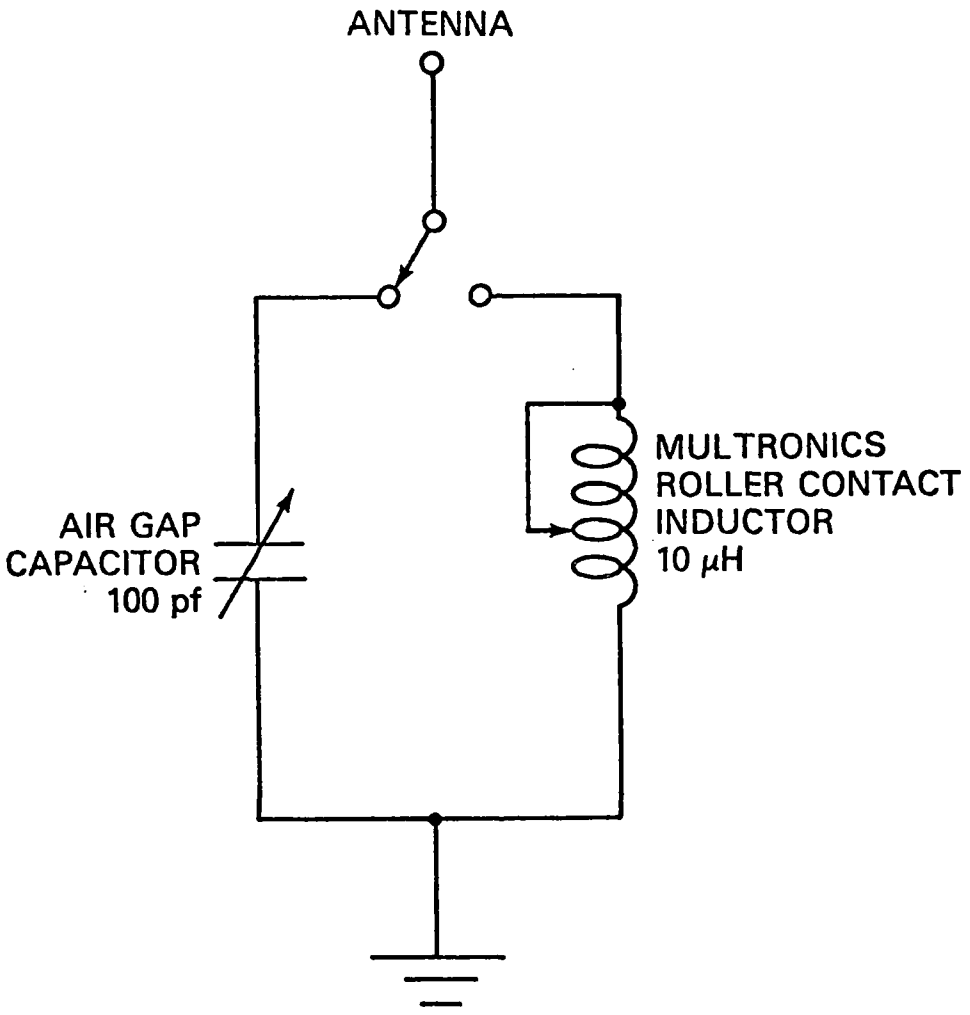

Fig. 3 — Adjustable reactance circuit quarter wavelength

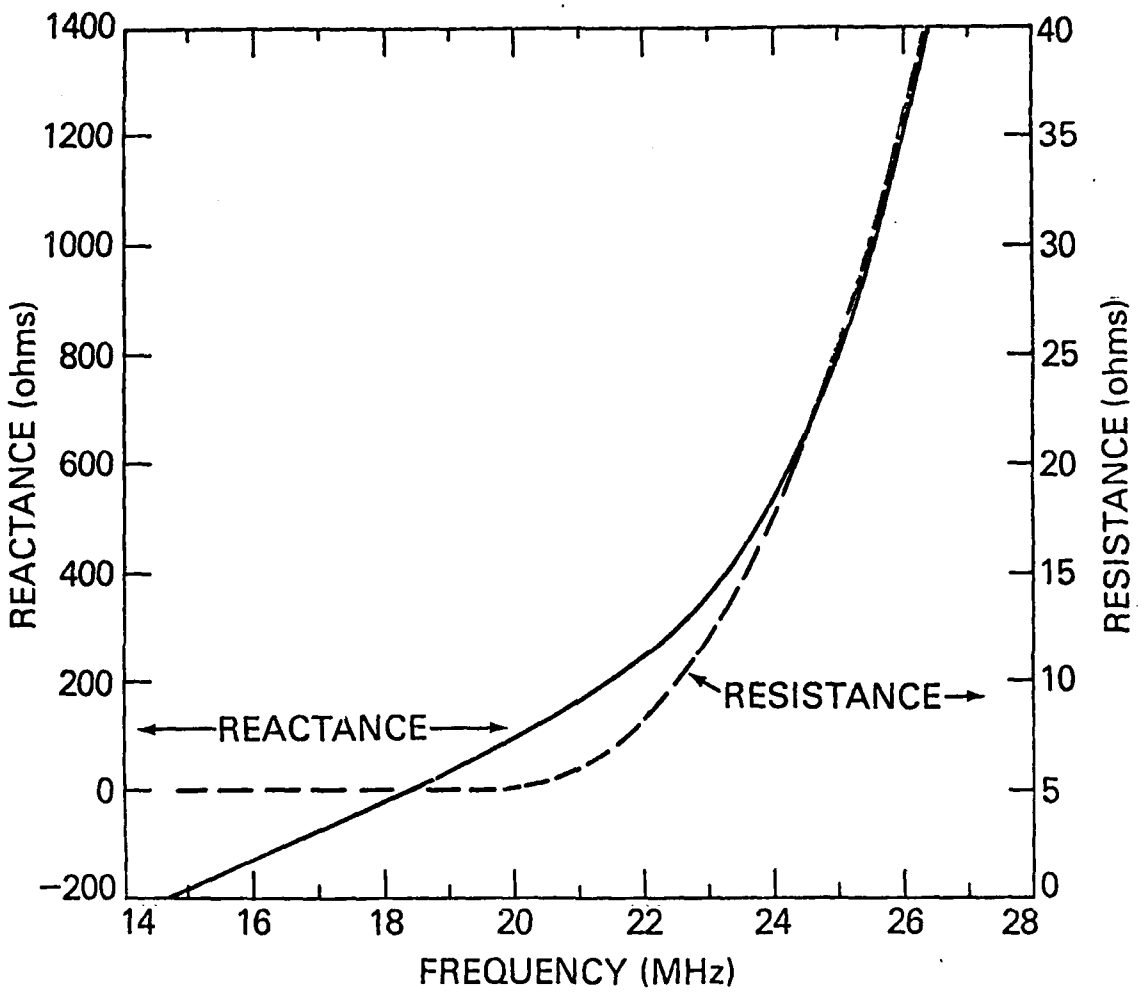

Fig. 4 — Impedance of the helically wound antenna element

Figure 5 is a photograph of the array, showing the central element and the surrounding parasitic elements. The spacing between the elements is 40 cm (0.024λ at the 18.4 MHz center frequency). The reactive loads are mounted in the boxes visible at the bottom of the parasitic elements; the circuit for the loads is presented in Fig. 6. The inductance is selected by the choice of inductors in the circuit (remotely switched by the relays shown), and continuous control of the reactance is obtained by adjusting the bias on a varactor diode. Figure 7 shows curves of reactance vs varactor bias voltage, which indicate that the reactance can be varied from -450 ohms to +450 ohms.

The effective height of the helical element at frequencies between 16 MHz and 25 MHz is shown in Fig. 8. The measured effective height is normalized to the effective height of a λ/4 monopole matched at each measurement frequency across this band. The helical element was matched at the center frequency (approximately 18.5 MHz) to the 50 ohm receiver input but was not changed for other frequencies.

IV. DETERMINISTIC PATTERN ADJUSTMENT

The array of matched λ/4 monopole elements, separated by a distance of λ/4, was evaluated in two different ways. In the first series of measurements, the pattern synthesis technique described by Luzwick and Harrington [6] was used to calculate the reactive loads required to produce a desired pattern. These calculated reactive loads were then set on the experimental antenna using a General Radio impedance bridge to monitor the impedance, and the radiation pattern was measured using a test signal generated by a 95 m distant souce. This approach can be called a "deterministic" technique to form the array pattern and is described in this section. In the second technique a azimuthally steered null was formed by observing the output of an HF receiver (see Fig. 2) when the 95 m distant source was radiating, and manually adjusting the reactive loads until the signal was minimized. This approach can be called an "adaptive" technique to form the array pattern and is discussed below in Section V.

We used the computer program listing given in Ref. 6 to generate the two sets of reactive loads listed in Table 1, as determined by the Rosenbrock algorithm. The desired pattern points and the patterns that resulted when these values were set on the reactive terminations are shown in Figures 9 and 10.

Fig. 5 — Experimental helical antenna

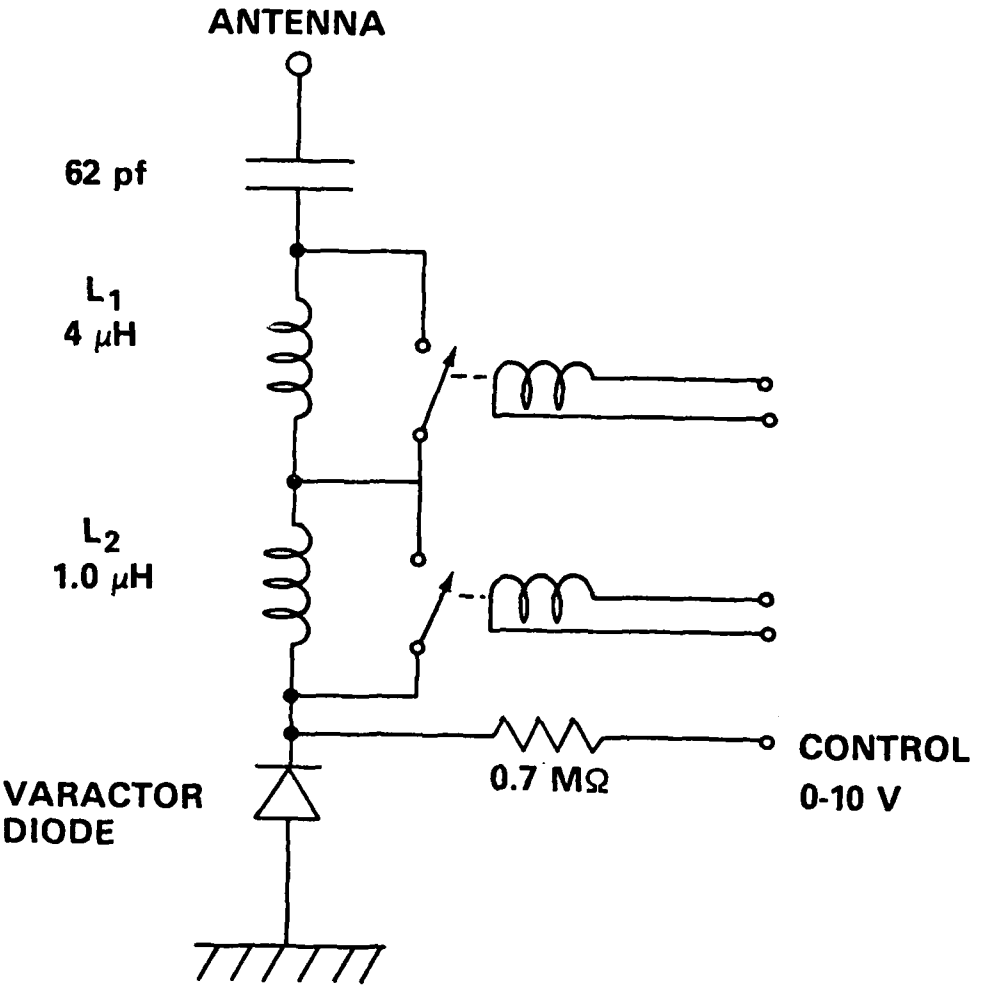

Fig. 6 — Adjustable reactance circuit for helical element array

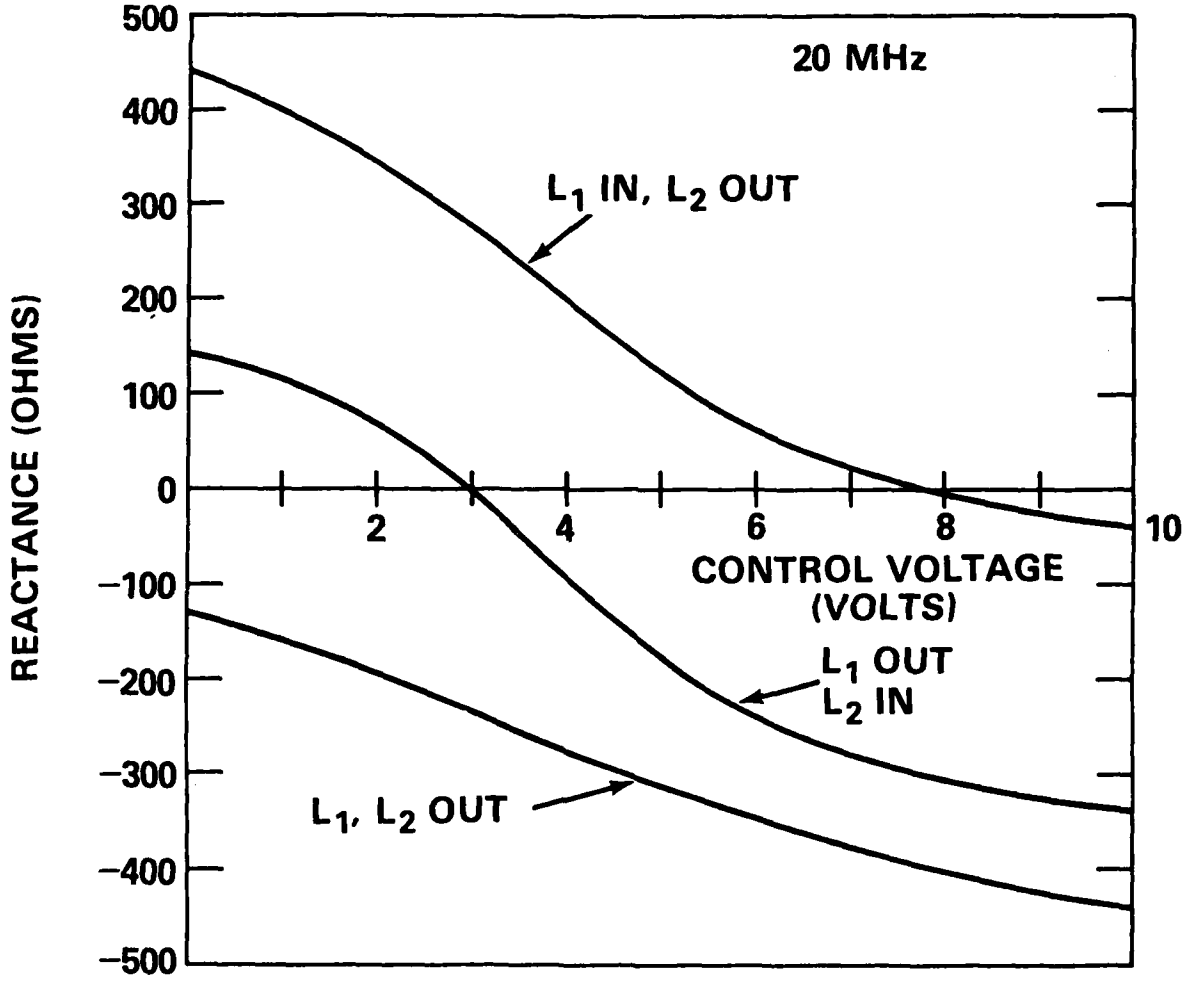

Fig. 7 — Reactance control characteristic, helical elements

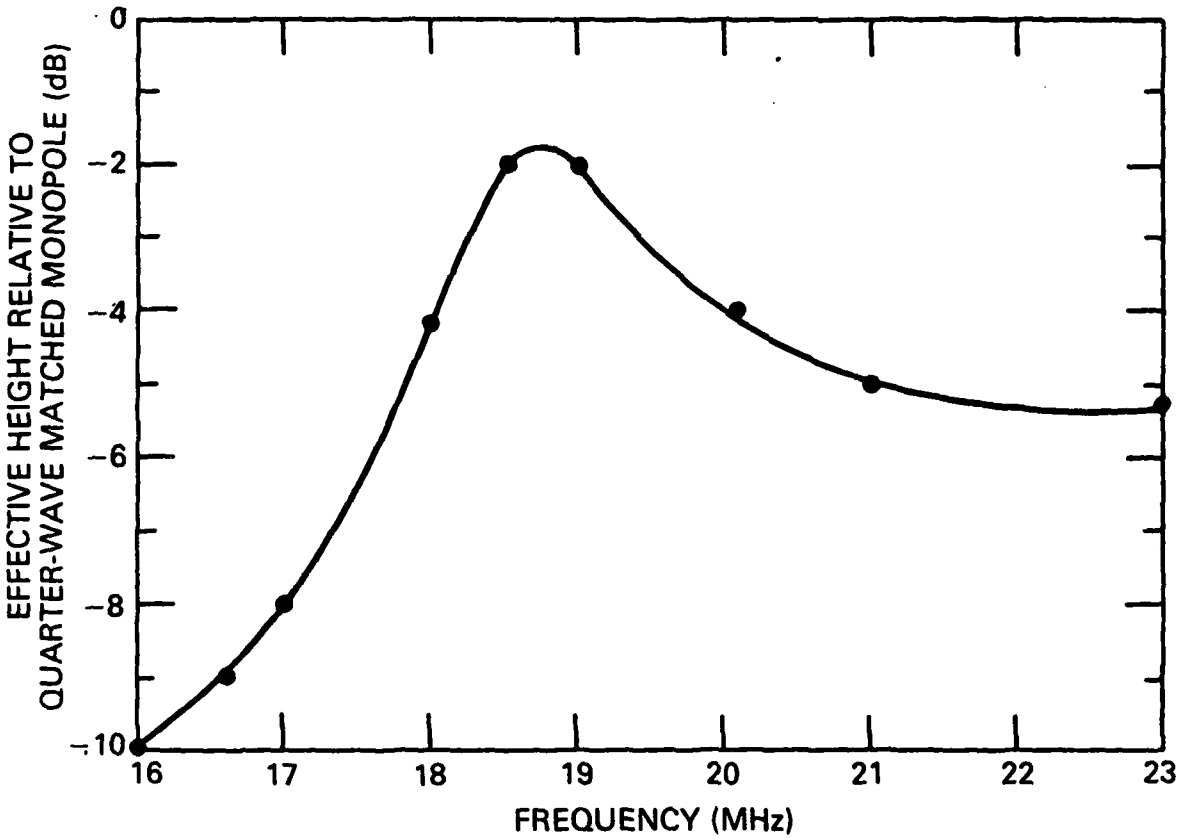

Fig. 8 — Helical element effective height

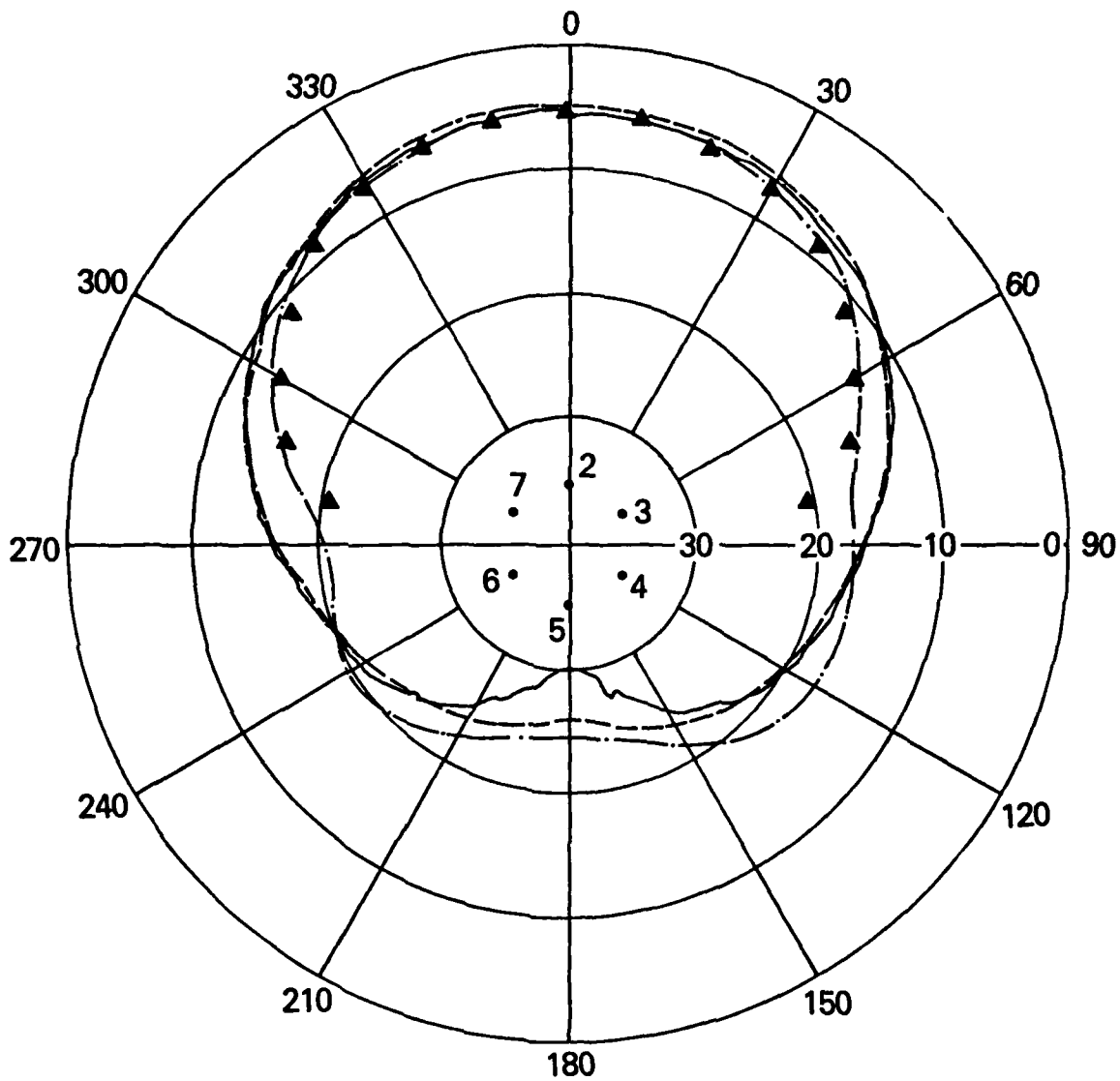

Fig. 9 — Synthesized patterns, quarter wave monopole array

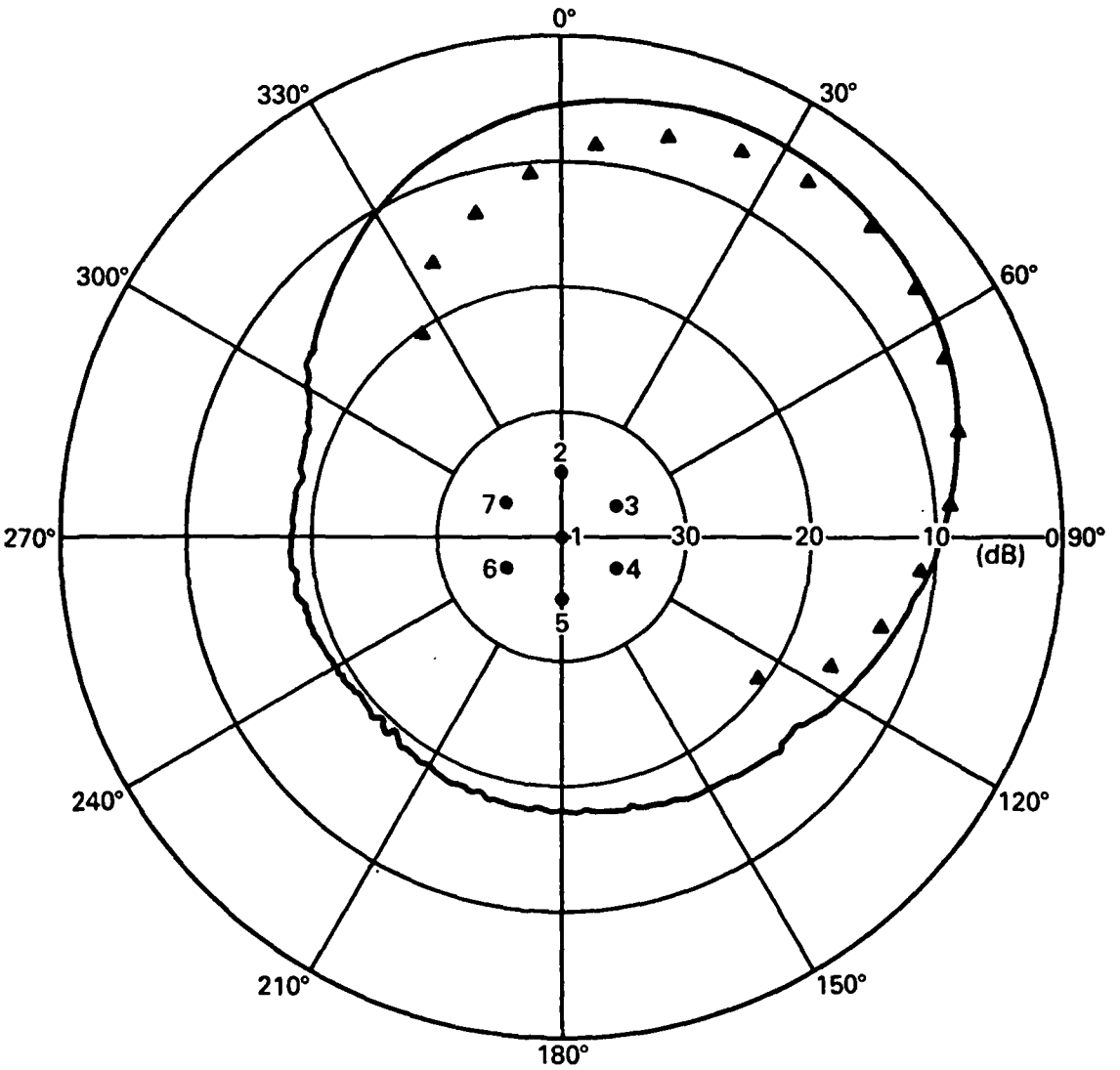

Fig. 10 — Synthesized patterns, quarter wave monopole array

Table 1. Values of loads (in ohms) for synthesized patterns.

Element Number	Pattern A	Pattern B
2	-52	-67
3	-58	-73
4	+45	-150
5	+ 7	+18
6	+45	+17
7	-63	-150

The desired pattern A in Table 1 has a lobe in a direction $\phi = 0^{o}$ with a 3 -dB beam width of about 100^{o} and has no side lobes. Figure 9 shows the results of three different trials at forming this pattern. The measured pattern has a lobe in the correct direction but has substantial side and back lobes. The three trials shown give an indication of the repeatability with which the reactive loads could be set. The General Radio bridge had a stated accuracy of at least one percent, but the stray inductance from the leads between the reactive load and the bridge, and the unavoidable influence of the bridge itself on the element coupling, limited the accuracy and repeatability of the reactive load setting.

The desired pattern B has a lobe in a direction $\phi = 45^{o}$ with the same beamwidth as pattern A. The measured pattern in Fig. 10 does have its main lobe rotated approximately 45^{o}, as expected, but by comparison with Fig. 9 the side and back lobes are substantially larger. The front-to-back ratio is only 15 dB for the lobe at 45^{o}, compared with 20 to 25 dB for the lobe at 0^{o}.

Other attempts at synthesizing a pattern in this manner by calculation of the required reactive loads produced generally similar results. Our conclusion is that the forming of a lobe with even moderate directivity is difficult because of approximations in the theory, the inability to set accurate reactance values for the loads, and the unavoidable resistive losses within the inductance coil. The impedance loads calculated from the theory assumed that the resistive portion of the impedance was small enough to be ignored, so that only a variable reactance was considered. Experimentally, however, we have measured the resistive portion of the impedance to vary between 2 to 6 ohms, depending on the value of the reactance. Resistance values of this magnitude have a definite effect on the pattern. Accounting explicitly for the resistive portion in calculating the loads, a step that might improve the agreement of experimental pattern and theory, is difficult because of the dependence of the resistive portion on the particular value of the reactance.

V. MANUAL ADAPTIVE ADJUSTMENT

Quarter-Wavelength Array Results

Figure 11 shows an example of the characteristic spatial notch pattern generated by nulling out an incident signal with adjustment of the reactive loads. The reactive loads were adjusted in no particular sequence; starting from random values of the reactances, each reactance was adjusted (one at a time) to produce a minimum in the receiver output and the process repeated until no further improvement was possible. The null in Fig. 11 is typical in shape, depth (at least 25 dB below the peak response), and width (about 50^{o} wide at points 3 dB below the peak response level) of nulls we were able to form in any arbitrary direction.

The response of only the single $\lambda/4$ center monopole (measured by opening the reactive loads on the parasitic elements) is omnidirectional and falls at a value of 5.0 dB on Fig. 11. Comparing this value with the array pattern, at azimuthal directions away from the null the array essentially has neither a positive nor negative gain relative to a monopole.

We made some additional measurements with the λ /4 monopole array, including bandwidth, nulling of more than one source, and measurements with smaller element separations. However, the results are essentially similar to those of the helical element tests discussed in the next section. The $\lambda/4$ monopole array served principally to illustrate that substantial azimuthal pattern control was possible with an array of parasitic elements. The need for an antenna element with more intrinsic inductance (so that the load inductors could be physically smaller) became evident during the λ /4 monopole measurements. Consequently, the array of helical elements was constructed and tested, as described in the next section.

Helical Element Results

1. Single Source Nulling

Figure 12 shows the spatial notch formed by adjusting the reactive loads to minimize an incident test signal. The antenna pattern is very similar to the pattern obtained in Fig. 11 with the $\lambda/4$ monopole array. Such a spatial notch could be formed in any arbitrary azimuthal direction. Also indicated in Fig. 12 is the equivalent receiver output for a single λ /4 monopole element, measured in a manner described below in the section that discusses the array sensitivity. There are two significant points to be made by Fig. 12. First, in spite of shrinking the overall diameter from 0.5λ (monopole array of Fig. 11) to $0.06\ \lambda$, the array is still able to form a rather sharp spatial notch. And secondly, the sensitivity of the array does not suffer any appreciable degradation, contrary to what might be expected for a very small array.

The reactive loads required to null a given incident wave are not unique, as demonstrated by Table 2. In this table, we present the results of five trials for adjustment of the reactive loads to null one signal incident at an angle of 0^{o}. Prior to each trial, the initial values of the reactive loads were randomized; the only difference in each trial is the reactive load chosen as the first one to vary in the search for the minimum. As is evident from the final values listed in the table, the

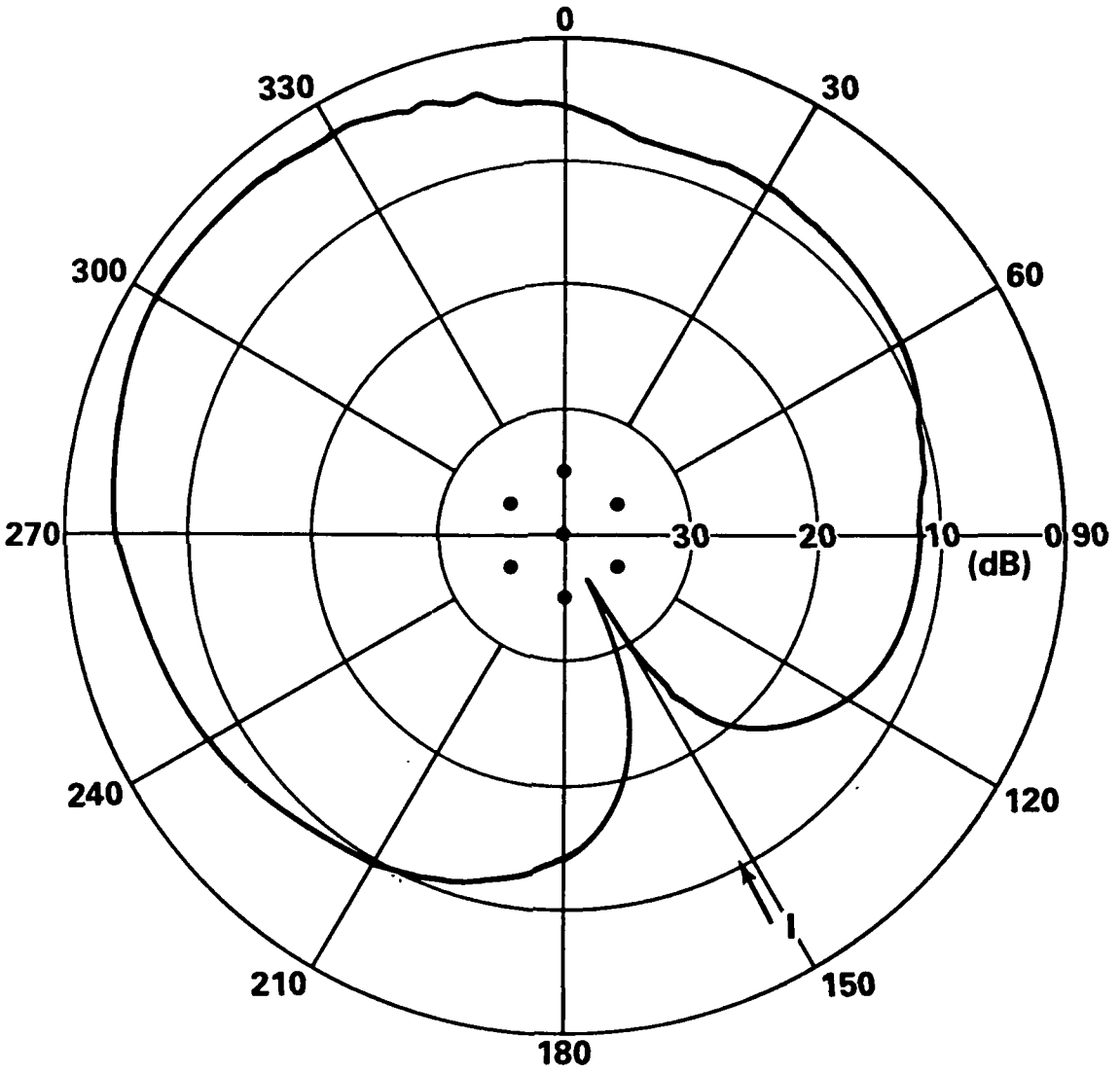

Fig. 11 — Adaptive null pattern, quarter wave monopole array

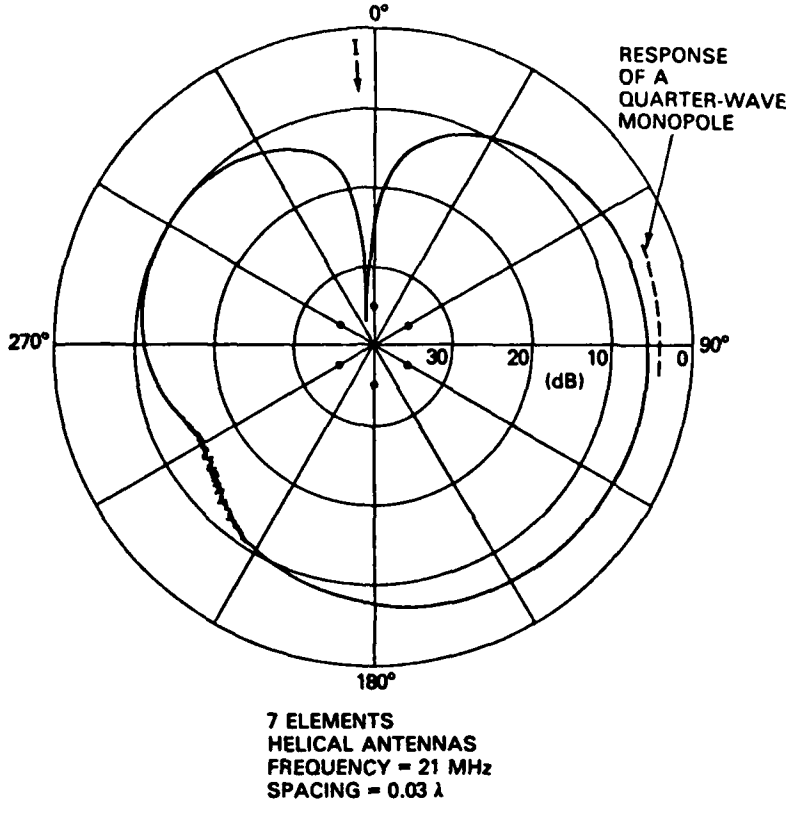

Fig. 12 — Adaptive null pattern, helical element array

signal can be nulled by many different combinations of reactive loads. In Fig. 13 we have shown the resulting patterns for each trial. Bear in mind that during the adjustment of the reactive loads the pattern is not monitored; only the receiver output is observed. The patterns in Fig. 13 are similar to each other, except that trial d produced a pattern with a second notch at 240°. The values of the reactive loads are almost all negative (capacitive) because at 21.5 MHz the antenna impedance is inductive (see Fig. 4).

Table 2. Results of Five Successive Trials to Null a Signal Incident at 0°

Trial No.	First Element Varied	Reactance Loads on Elements (ohms)					
		2	3	4	5	6	7
a	2	-340	-265	-350	-225	-100	-180
b	3	32	30	-320	-240	-350	-170
c	4	-230	-160	-350	-220	-315	5
d	6	-235	-225	-400	-360	-215	-365
e	7	-200	-235	-350	-190	-205	-240

2. Signal-to-Interference Ratio (SIR) Maximization

In one anticipated application of a reactively steered array a main lobe would be steered towards a desired signal and simultaneously nulls would be steered towards one or more interfering sources. The feasibility of this application was investigated in the present work using manual adaptation, and the results are described in this section.

The method used to derive an array output proportional to the SIR is shown in Fig. 14. The incident desired signal and the interference signals were slightly offset in frequency ($\sim$1 kHz), so that they all fell within the 16 kHz bandwidth of the receiver but were separated sufficiently that a subsequent narrowband filter (10 Hz bandwidth) could be tuned only to the desired signal. The 455 kHz IF output of the receiver was heterodyned to a frequency of 50 kHz and passed through two stages of hard limiting. The limiter output was applied to a lock-in detector functioning as a 10 Hz narrowband filter tuned to the frequency of the desired signal. The in-phase output of the lock-in was displayed on an oscilloscope and a rms voltmeter. Because of the suppression factor of a limiter, the output of the lock-in detector is proportional to SIR, as long as SIR $<<$ 1. Thus, the array can be adjusted in its initial stages using this approach, when the interference is much larger than the signal. However, as the array adapts and the SIR approaches unity, the output becomes insensitive to SIR; but, at that point, the signal can be discerned from the interference, and adjustment of the loads to maximize the signal alone without the limiter can continue to improve the SIR. The use of a hard limiter in this manner is convenient to demonstrate the pattern forming ability of the array but may not be practical in an eventual application.

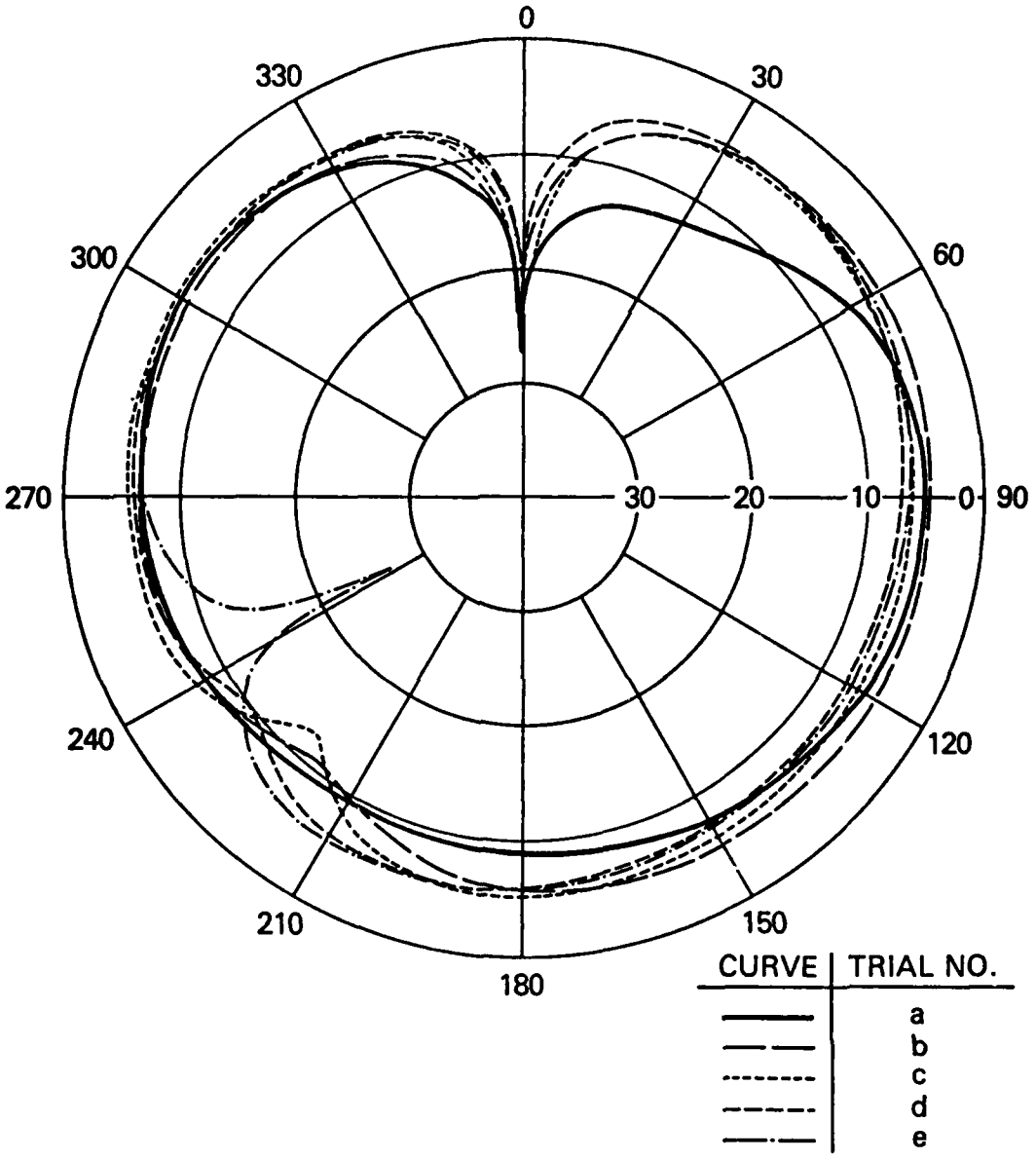

Fig. 13 — Adaptive patterns resulting from five independent trials

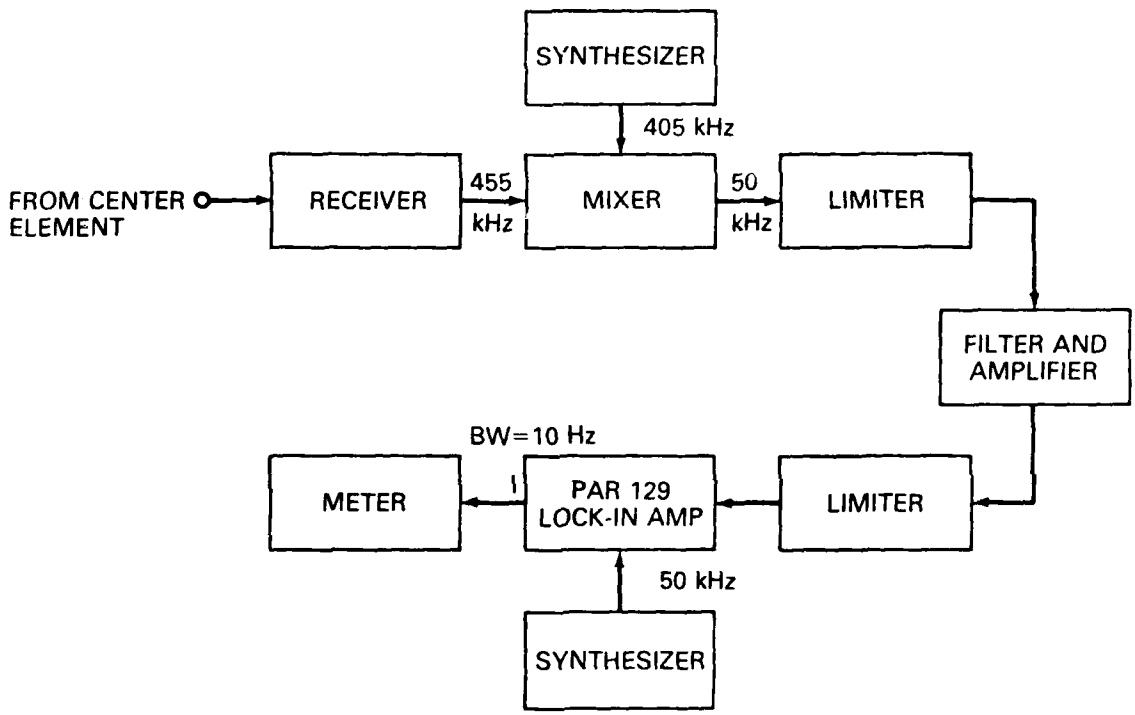

Fig. 14 — Signal-to-interference ratio detector

Figure 15 shows an example of a desired signal at 0° and a single interferer at 20°. The initial reactive loads were randomized, and the received field strength of the interferer was 20 dB higher than the desired signal. The reactive loads were then adjusted to maximize the monitored output voltage, and the resulting pattern is shown. A notch has formed in the direction of the interferer, and to the maximum extent possible the pattern lobe has pointed itself in the direction of the desired signal. The SIR after adaptation is about 0 dB, i.e., the notch depth is 20 dB below the pattern gain in the direction of the desired signal. The signal-interferer separation of 20° shown in Fig. 15 represents the minimum separation for which we have been able to maximize the SIR.

In Figure 16 we present the adapted pattern for a desired signal and two interferers. For each interferer, SIR = -20 dB. Again, the pattern has adjusted itself to place a null on each interferer and a lobe on the desired signal.

The results in Figs. 15 and 16, we emphasize, are typical and do not represent any special cases in which particularly good pattern adjustment was achieved. The adjustment of the reactive loads in these two cases was performed in no specific order; the loads were iteratively adjusted until no further improvement was possible, a procedure that usually took 2 to 3 minutes. Below in Section VI, we discuss an algorithm by which the adapted patterns can be formed manually in only a few seconds and that has the potential with microprocessor control for adaptation times on the order of milliseconds.

3. Bandwidth and Frequency Response

The bandwidth of the array can be defined in several ways, and we choose the following approach. Using a single monochromatic source representing an interferer, the reactive loads were adjusted to obtain a null. These loads were then left untouched, and the source frequency and receiver center frequency were shifted in lockstep. The pattern was measured to observe the manner in which the depth of the null changed with frequency. The bandwidth of the array then is the frequency range over which the null depth (relative to the main lobe) remains below a specified value.

Figure 17 displays the patterns measured for loads set at 21.505 MHz as the frequency of the source varies between 21.48 MHz and 21.55 MHz. In Fig. 18 we have plotted the null depth below the main lobe level as a function of frequency. Somewhat arbitrarily we select a 20 dB null depth as a point at which to measure the bandwidth; the nulling bandwidth is thus found to be about 40 kHz.

We define the frequency response to be the frequency range over which we can use the array to form a null (on a CW signal) that is at least 20 dB below the main lobe response. For our array with elements tuned to 18.5 MHz, the upper frequency limit is determined by the pole in the antenna element frequency response near 28 MHz evident in Fig. 4. As the frequency increases, the inductive reactance increases to the point where a capacitive reactance load cannot compensate; in addition, the resistive component

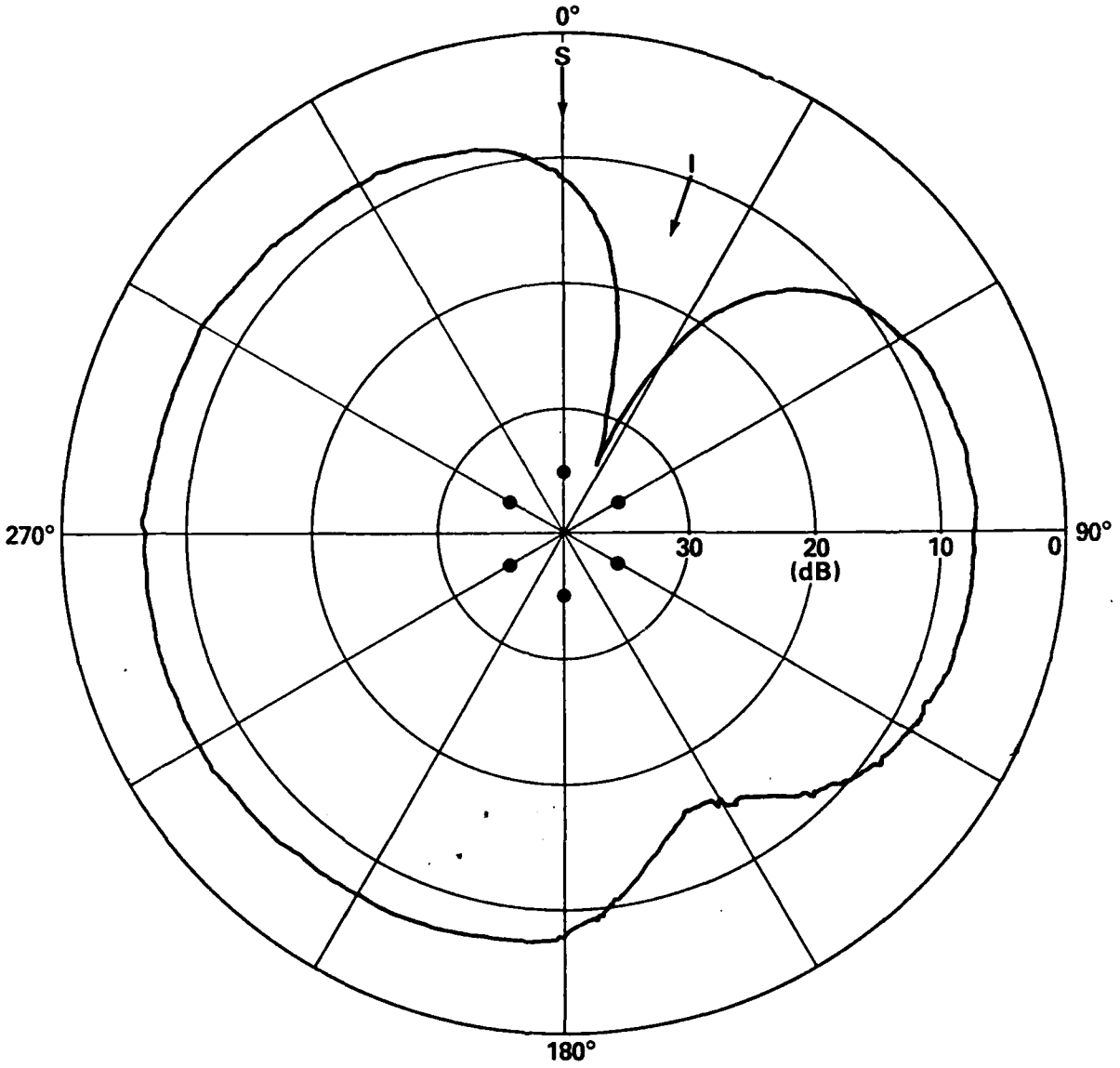

Fig. 15 — Adaptive array performance, signal plus one interferer

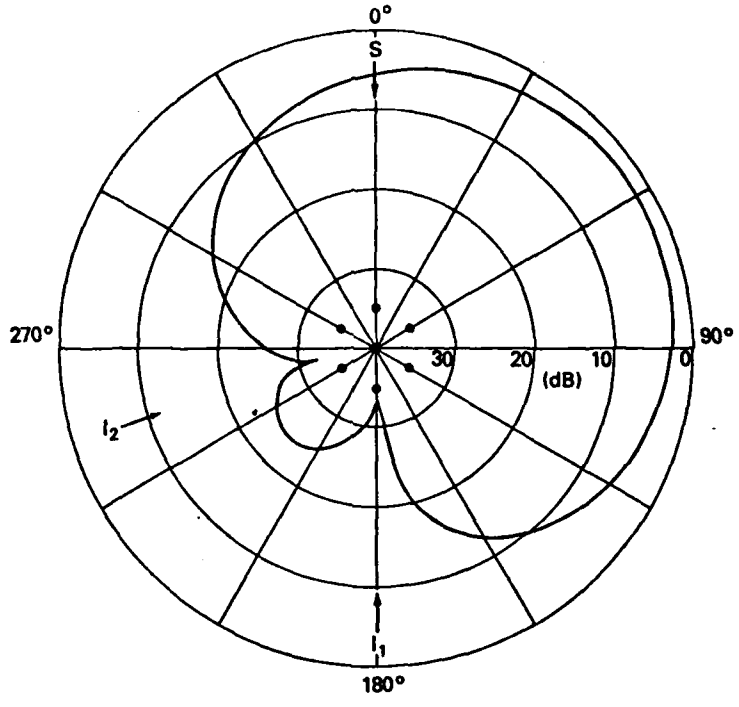

Fig. 16 — Adaptive array performance, signal plus two interferers

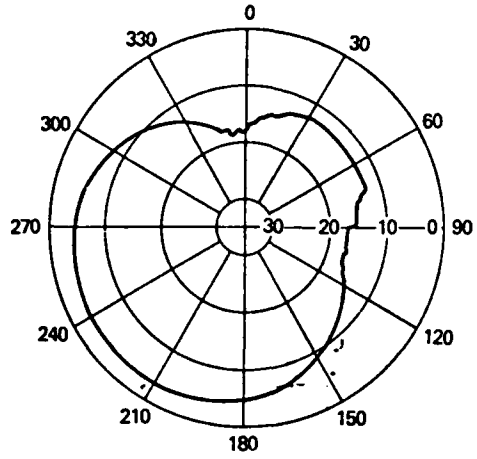

FREQUENCY = 21.48 MHz

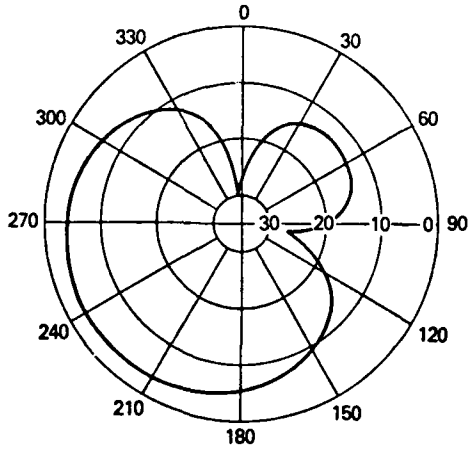

FREQUENCY = 21.495 MHz

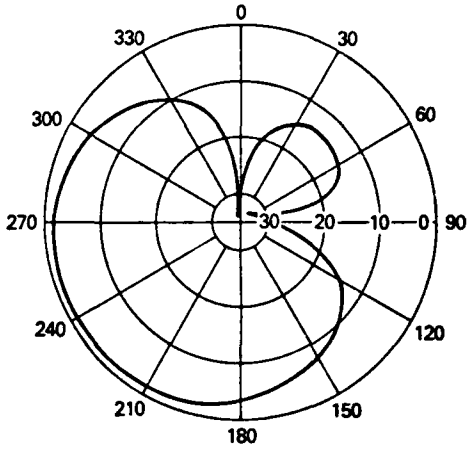

FREQUENCY = 21.51 MHz

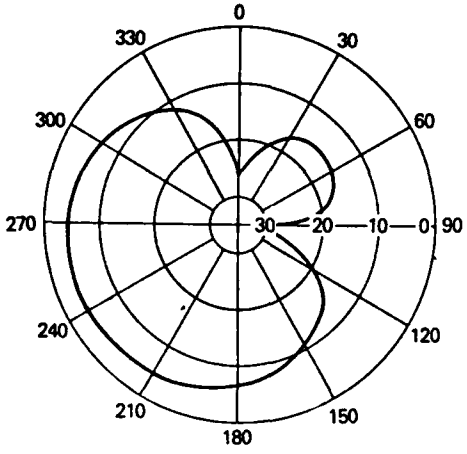

FREQUENCY = 21.53 MHz

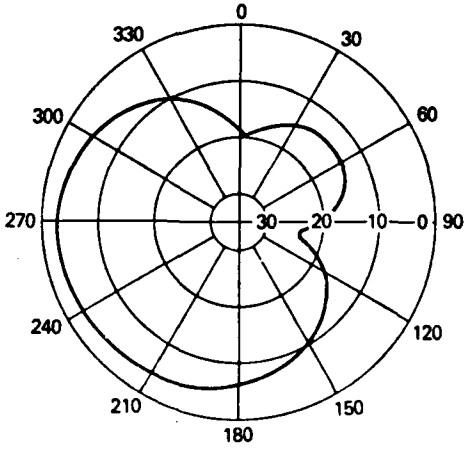

FREQUENCY = 21.54 MHz

Fig. 17 — Frequency dependence of antenna pattern for a fixed adaptive solution

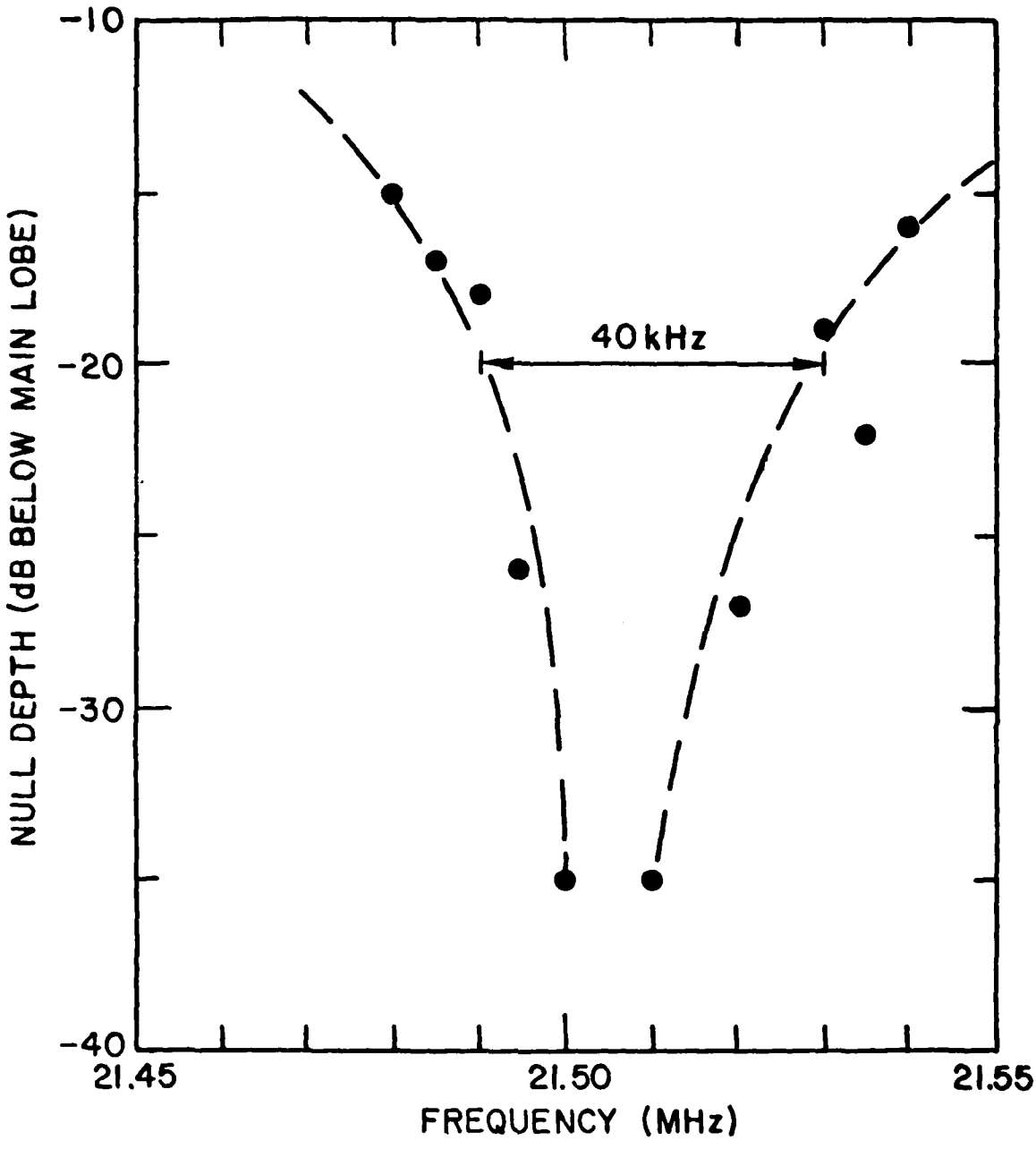

Fig. 18 — Frequency dependence of null depth for a fixed adaptive solution

increases and affects the pattern. By the impedance curve in Fig. 4 the element inductive reactance curve equals the maximum possible load capacitive reactance of about -500Ω at a frequency of 25 MHz. We indeed observe that at about 25 MHz and higher we do not have enough adjustment range in some of the reactive loads to null out an incident signal. The resistive losses also begin to decrease the array sensitivity at 25 MHz.

The lower frequency limit is determined by the point at which the wavelength of the signal is so large relative to the array element spacing that the wave incident on the center element and the waves reflected by the parasitic elements are unresolvable. That is, the phase diameter of the array becomes very small. We observe this effect as a "touchiness" of the reactive loads, whereby a small change in the varactor control voltage has a large effect on the pattern. This onset occurs at a frequency of about 15 MHz with our existing manually controlled array. The implementation of an automatic control algorithm (see Section VI) will probably permit a somewhat lower frequency of operation because the minimization point can be searched more accurately and with finer resolution.

4. Array Sensitivity

A well-known consequence of decreasing the size of an array is an increase in the ohmic losses and a decrease in the array radiation resistance. For a receiving array this manifests itself as a decrease in the open circuit voltage at the antenna terminals.

The array sensitivity was determined by first measuring the effective height of a single helical element and comparing the value with the effective height of a quarter-wave monopole. This measurement was presented in Section III. Then, during the pattern measurements, a measurement of the pattern was made with all reactive loads open. This pattern was always omnidirectional and was identical to the pattern that would be obtained if all of the parasitic elements were physically removed from the array. This omnidirectional pattern level thus calibrated the array pattern against the effective height of a single helical element, which in turn had previously been calibrated against a standard quarter-wave monopole.

The response level corresponding to a $\lambda/4$ monopole has been indicated for most of the antenna patterns presented above. In general the main lobe of the patterns falls about 5 dB below the $\lambda/4$ monopole response. Since the effective height of the helical element at its center frequency is about 2 dB less than a $\lambda/4$ monopole (see Section III), the arraying of the elements introduces a decrease of about 3 dB in the maximum antenna gain near the 19 MHz resonant frequency. In the HF band the ambient noise temperature exceeds the receiver noise temperature by many tens of dBs, so that a loss of 3 dB in antenna sensitivity due to arraying is of no practical consequence.

VI. AN EMPIRICALLY-DEVELOPED CONTROL ALGORITHM

It is not clear to us yet if the adaptive control methods [8] commonly used for conventional antenna arrays (i.e., those arrays that employ a summing device), such as the Widrow least mean squares algorithm or the

Howells-Applebaum algorithm, can be modified for a reactively steered array. We have, however, developed an algorithm based on our experience with manual adjustment of the array that appears to be suitable for eventual rapid automatic control for interference nulling.

The technique makes use of a sawtooth ramp applied to the varactor bias voltage of one of the reactive loads. The voltage sweeps the reactive load through its range of values; the output of the array receiver then always displays a minimum at some bias voltage value.

Figure 19 is a flow chart of an algorithm that uses the ramped varactor bias voltage in a systematic manner to steer pattern nulls in the direction of interferers. Shown to the right of the flow chart are drawings taken from oscilloscope photographs of the waveform of the receiver output at each point in the adjustment process. The sawtooth ramp is applied first to any arbitrary reactive load (in Fig. 19 element 2 has been selected) and the other reactive loads are adjusted in turn to minimize the value of V_o. In many cases only several loads have to be adjusted to bring V_o less than V_n (V_n = a threshold voltage at which cancellation is deemed to be sufficient). Occasionally, depending on the angle of incidence of the interference, the first load selected for ramping does not permit the condition $V_o < V_n$ to be attained, and Fig. 19 allows for this circumstance by indicating that another load is then ramped and the adjustment process repeated. We have never encountered a situation in which more than two loads had to be ramped. This technique works well with one or two sources of interference. The technique has been used equally successfully both for nulling of incident interferers and for maximization of a SIR output.

The eventual adaptation speed that can be realized with computer control will depend on the rate at which the varactor diodes can be ramped, on the cycle time of the microprocessor for executing the algorithm instructions, and on the receiver bandwidth (for adaptive control at the IF). The 7 μs time constant for the varactor diode bias circuit allows a ramp rate of at least 100 kHz, but the 16 kHz or less receiver bandwidths typical at HF would permit ramp rates (for a relatively undistorted signal) of only a few kHz. Typical microprocessor cycle times are 5 μs or less, even for relatively complex instructions, so that during a single ramp period of a 2 kHz ramp, at least 100 operations could occur. This number of operations is sufficiently large that a complex minimum seeking algorithm can be implemented. Hence, assuming an average of 5 sweeps of the ramp to minimize each of 6 loads, the adaptation time for a 2 kHz ramp rate is (1/2000)(5)(6) = 15 ms, if only one load has to be ramped. Proportionally faster adaptation times could be achieved for larger IF bandwidths.

VII. SUMMARY AND CONCLUSIONS

Measurements have been made on two 7 element azimuthally-symmetric arrays, with one active receiving element mounted at the center of six symmetrically positioned parasitic elements with variable reactive loads. One array used $\lambda/4$ monopole elements with a spacing between the elements of 3.60 m ($\lambda/4$ at 21 MHz), and the other array used helically-wound elements with a physical height of 1.3 m and a spacing between the elements

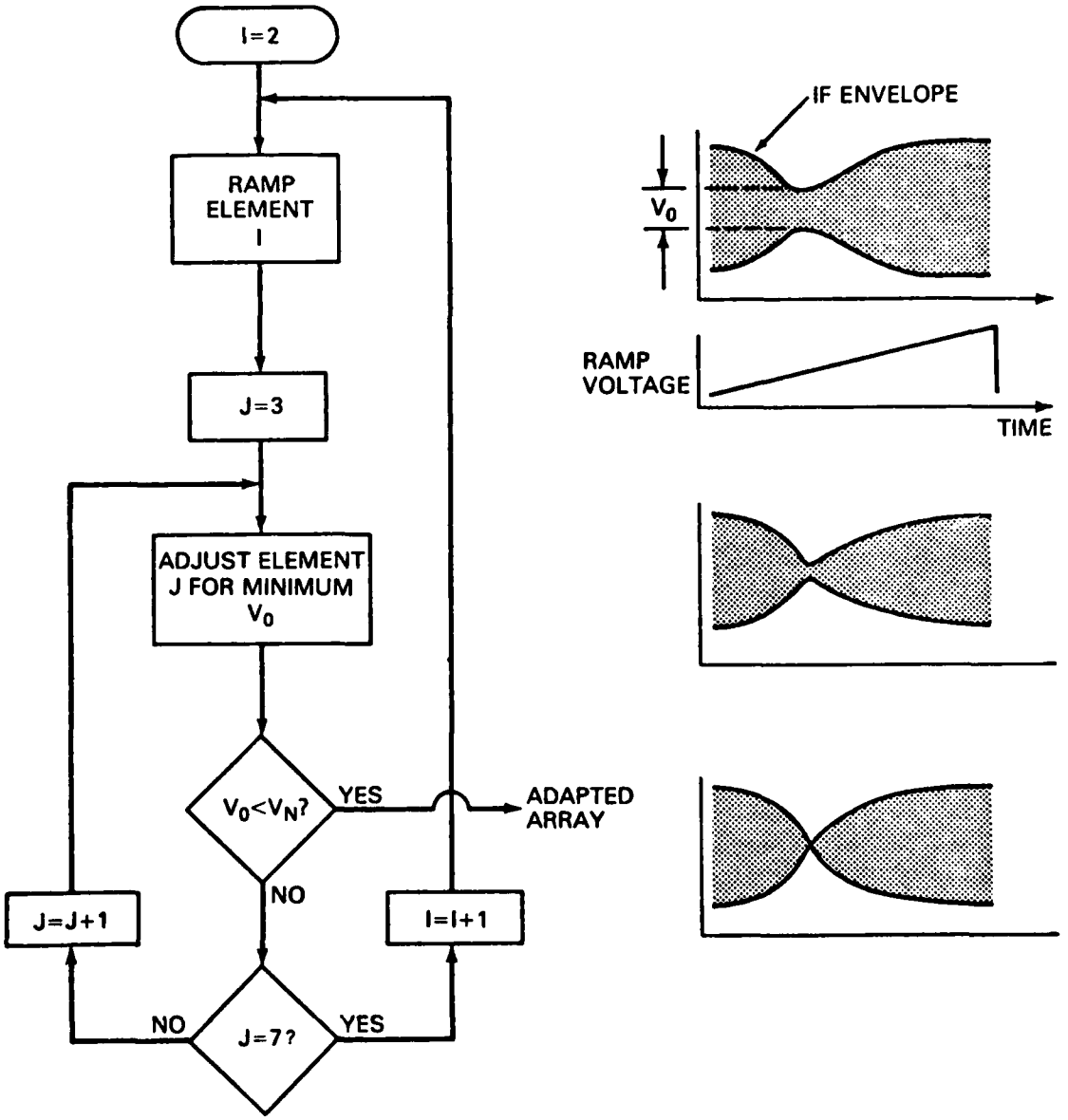

Fig. 19 -- Simple adaptive algorithm

of 40 cm (0.024λ at the 18.4 MHz center frequency). Most of the measurements reported here used the arrays in an "adaptive" mode, in which the reactive terminations were adjusted (manually) to minimize one or two incident signals representing undesired interference, or to maximize a processed receiver output proportional to S/I, where S is a desired signal incident on the array and I is total interference. The manual adaptation consistently produced sharp spatial notches in an otherwise nearly omnidirectional pattern in the direction of two interferers; the notches typically had a width of 50 degrees and a depth of 25 to 30 dB below the pattern main lobe. The cancellation bandwidth was usually at least 40 kHz. The manual adaptation used essentially an univariate search approach to produce the nulls and was necessarily slow; the manual adaptation served principally to demonstrate the potential of the reactively steered array. An algorithm that uses a ramp voltage to dither the reactive loads appears to be implementable in a microcomputer for rapid automatic adaptive control of the array, and the array is presently being interfaced to a PDP-11/03 computer to evaluate this algorithm.

Attempts were made to form the array pattern deterministically by using Harrington's theory to compute the reactive loads necessary to form a pattern lobe in a given direction. Although the pattern lobe could be steered in the general desired direction, the directivity of the pattern was low and reproducibility poor. We conclude that deterministic pattern forming with a reactively steered array is difficult to achieve.

The very small overall size of the reactively steered HF array with helical elements makes it particularly attractive for applications on ships and aircraft where space for a conventional array with element separations of $\lambda/2$ or larger is not available. The primary drawback of the array, at present, is the relatively small frequency response range of 15 MHz to 25 MHz; however, the lower limit can possibly be extended downward by using more precise automatic control of the array. Also, since the array is compact, multiple arrays can be realistically considered to cover the entire 3 to 30 MHz HF band.

REFERENCES

1. Harrington, R.F., "Reactively Controlled Directive Array", IEEE Transactions on Antennas and Propagation, VAP-26, No. 3, pp 390-395, 1978.

2. Vagi, H., "Beam Transmission of Ultra Short Waves", Proceedings IRE, V. 16, pp 715-741, 1928.

3. Zeger, A.E., Wismer, L.D., Dinger, R.J., "Adaptive Control of Parasitic Elements", Proceedings of the 1980 Adaptive Antenna Symposium, pp 87-105, RADC Report No. TR-80-378, V. 1, December 1980.

4. Harrington, R.F., Wallenberg, R.F., Harvey, A.R., "Design of Reactively Controlled Antenna Arrays", Technical Report No. 4, Department of Electrical & Computer Engineering, Syracuse University, September 1975.

5. Luzwick, J., Harrington, R.F., "Pattern Magnitude Synthesis For a Reactively Loaded Circular Antenna Array", Technical Report No. 6, Department of Electrical & Computer Engineering, Syracuse University, August 1977.

6. Luzwick, J., Harrington, R.F., "A Comparison of Optimization Techniques as Applied to Gain Optimization of a Reactively Loaded Linear Array", Technical Report No. 1, Department of Electrical & Computer Engineering, Syracuse University, February 1976.

7. Rosenbrock, H.H., "An Automatic Method of Find the Greatest or Least Value of a Function", The Computer Journal, V. 3, pp 175-184, October 1960.

8. Gabriel, W.F., "Adaptive Arrays - An Introduction", Proceedings of the IEEE, V. 64, pp 239-272, February 1976.